Transport parameters in neutron stars from in-medium NN cross sections

H. F. Zhang,[1] U. Lombardo,[2] and W. Zuo[3]
[1]*School of Nuclear Science and Technology, Lanzhou University, Lanzhou 730000, People's Republic of China*
[2]*Dipartimento di Fisica and INFN-LNS, Via S. Sofia 64, I-95123 Catania, Italy*
[3]*Institute of Modern Physics, Chinese Academy of Sciences, Lanzhou 730000, People's Republic of China*
(Received 7 April 2010; revised manuscript received 15 June 2010; published 15 July 2010)

We present a numerical study of shear viscosity and thermal conductivity of symmetric nuclear matter, pure neutron matter, and β-stable nuclear matter, in the framework of the Brueckner theory. The calculation of in-medium cross sections and nucleon effective masses is performed with a consistent two- and three-body interaction. The investigation covers a wide baryon density range as needed in the applications to neutron stars. The results for the transport coefficients in β-stable nuclear matter are used to make preliminary predictions on the damping time scales of nonradial modes in neutron stars.

DOI: 10.1103/PhysRevC.82.015805 PACS number(s): 97.60.Jd, 26.60.−c, 21.65.−f

I. INTRODUCTION

Neutron stars are a unique laboratory for studying the equation of state of nuclear matter at high density and isospin asymmetry, beyond the ranges typical of heavy-ion collisions and nuclei far from stability. But the observation data are still far from uniquely constraining the properties of exotic states of nuclear matter. The detection of gravitational waves could push forward the field of neutron star physics. As the gravitational waves drive the instability of neutron star oscillations, including nonradial modes, the possible damping mechanisms have to be investigated to justify the existence of rapidly rotating stars. Good candidates are the viscosity and the thermal conductivity of the neutron star constituents. The important role that these parameters can play is the main reason for the uninterrupted interest in the transport theory of dense matter over the past three decades [1]. Microscopic models of nuclear matter (i.e., based on bare interactions) have been faced with the interpretation of the equilibrium properties of neutron stars, such as their structure [2] and the onset of superfluidity [3]. The same theoretical models have been also applied to calculate effective mass [4] and medium renormalized nucleon-nucleon (NN) cross sections [5], both extensively used in the transport-model simulations of heavy-ion collisions. But only recently were these two quantities redirected to describe the transport properties of nuclear matter. These quantities are in fact the main ingredients for calculating the viscosity and thermal conductivity coefficients in neutron stars. The extension of such calculations to regimes of high density and isospin, needed in the study of neutron matter cores, together with the interpretation of their inner structure, is a main challenge for current microscopic theories of nuclear matter.

So far all calculations based on microscopic many-body approaches with realistic interactions have shown that the medium effects result in a noticeable suppression of the NN cross sections σ_{NN} [5] and, as a consequence, in an enhancement of both shear viscosity and thermal conductivity. Calculations in dense nuclear matter have been performed in the T-matrix approach [6], in the correlated basis function (CBF) approach [7], and in the Brueckner-Hartree-Fock (BHF) approximation [8]. Calculations of the transport coefficients in β-equilibrium nuclear matter have been performed with the equation of state (EoS) of asymmetric nuclear matter from the variational approach [9,10], and from the CBF approach [11]. Despite the overall agreement on the medium effects, different approaches could give different predictions for transport parameters in β-equilibrium nuclear matter since they differ from each other in the isospin dependence, which becomes more and more visible at higher density. The results should be insensitive to the choice of the two-body potential because all realistic potentials used in the microscopic calculations are accommodated on the experimental NN scattering phase shifts. But a dependence is expected on the three-body force, especially at high density, where its influence on the EoS is dominant. Therefore, it seems interesting to compute the shear viscosity and the thermal conductivity of nuclear matter, especially β-stable nuclear matter, in a wide range of densities needed for the study of the neutron star core. This will be done within the BHF approximation. The latter embodies, within a unified meson-exchange model framework, two- and three-body forces. The meson parameters of the two-body realistic interaction (the Bonn B [12] in our case), which fit the experimental NN scattering phase shifts in vacuum, are also adopted to describe the three-body force [13]. In this paper the numerical results will be tested, within the simple model of a constant-density neutron star, on the calculation of the dissipation time scales to be compared with the time scale of emitting gravitational radiations.

II. TRANSPORT PARAMETERS

The transport parameters of Fermi liquids were derived by Abrikosov and Khalatnikov (AK) from the Landau kinetic equations for a multicomponent system [14],

$$\frac{\partial f_i}{\partial t} + \{f_i, \epsilon_p\} = \sum_k \mathcal{I}_{ik}, \tag{1}$$

where $f_i(\vec{r}, \vec{p})$ is the quasiparticle distribution of the component i, ϵ_p is the quasiparticle energy, and $\mathcal{I}_{ik}$ is the collision integral between particles of components i and k. From the linearization of the kinetic equations, the shear

viscosity η and thermal conductivity κ can be extracted in the AK approximation. The exact expressions, obtained by Brooker and Sykes after revisiting the resolution of the kinetic equations [15,16], are written as follows:

$$\eta T^2 = \tfrac{1}{20}\rho v_F^2 W(\rho) C(\lambda), \tag{2}$$

$$\kappa T = \tfrac{1}{12} v_F^2 p_F W(\rho) H(\mu), \tag{3}$$

where

$$W^{-1}(\rho) = \frac{1}{2\epsilon_F}\int_0^{4\epsilon_F} dE \int_0^{2\pi} \frac{d\theta}{2\pi} \frac{1}{\sqrt{1 - E/4\epsilon_F}} \sigma(E,\theta), \tag{4}$$

with ρ the density, $v_F = p_F/m^*$ the Fermi velocity, and m^* the effective mass. and where $C(\lambda)$ and $H(\mu)$ are correction factors corresponding to the exact solution (for details see Refs. [15,16]). The key quantity is the in-medium cross section, here expressed in terms of the energy E in the laboratory frame and the scattering angle θ in the center-of-mass frame. The upper limit of the energy integration in the average cross section is four times the Fermi energy of a free Fermi gas, $\epsilon_F = p_F^2/2m$, owing to the approximation of restricting the nucleon excitations around the Fermi surface. As described in the following, the in-medium cross sections are calculated within the Brueckner theory.

III. IN-MEDIUM CROSS SECTIONS FROM THE BRUECKNER THEORY

In the interior of a neutron star the hadron density can reach values several times the nuclear matter saturation density, so that the nucleon-nucleon (NN) collisions are expected to be deeply affected by the surrounding medium and the corresponding cross sections can be quite different from those in free space. There are two main medium effects. First, the NN scattering amplitude is dominated by the S-wave components of the effective interaction so that a flattening of the angular distribution is expected in comparison with the free cross section, which, in the center-of-mass frame, is peaked in the forward and backward directions. Second, the level density in the entrance and exit channels gets reduced by the strong medium renormalization of the effective mass.

Both effects can be well described in the framework of the self-consistent Brueckner theory. In the past few years the latter has made a remarkable step forward by means of the three-body force, introduced not only to reproduce the empirical saturation properties of nuclear matter but also to extend the calculations to high density. The Brueckner theory with two- and three-body forces is described elsewhere [17,18]. Here we simply give a brief review of the BHF approximation, adopted for the present calculations. The starting point is the reaction G matrix, which satisfies the Brueckner-Bethe-Goldstone (BBG) equation,

$$G(\omega) = v_{NN} v + v_{NN} \sum_{k_1 k_2} \frac{|k_1 k_2\rangle Q_{k_1,k_2} \langle k_1 k_2|}{\omega - \epsilon_{k_1} - \epsilon_{k_2}} G(\omega), \tag{5}$$

where $k_i \equiv (\vec{k}_i, \sigma_i, \tau_i)$ denotes the single-particle (s.p.) momentum, the z component of spin and isospin, respectively, and ω is the starting energy. The G matrix, the Pauli operator Q, and the s.p. energies $\epsilon_k = k^2/2m + U_k$ depend separately on the neutron and proton densities. The interaction v_{NN} given by

$$v_{NN} = V_2^{\text{bare}} + V_3^{\text{eff}}, \tag{6}$$

where V_2^{bare} is the bare two-body force and V_3^{eff} is the three-body force averaged on the third particle as follows:

$$\begin{aligned}\langle \vec{r}_1\vec{r}_2|V_3^{\text{eff}}(T)|\vec{r}_1{}'\vec{r}_2{}'\rangle &= \frac{1}{4}\mathrm{Tr}\sum_n \int d\vec{r}_3 d\vec{r}_3{}' \phi_n^*(\vec{r}_3{}')[1-\eta(r_{13}')][1-\eta(r_{23}')] \\ &\times W_3(\vec{r}_1{}'\vec{r}_2{}'\vec{r}_3{}'|\vec{r}_1\vec{r}_2\vec{r}_3)\phi_n(r_3)[1-\eta(r_{13})][1-\eta(r_{23})].\end{aligned} \tag{7}$$

Since the defect function $\eta(r)$ [where $1-\eta(r)$ is the correlated two-body wave function] is directly determined by the solution of the BBG equation [17], V_3^{eff} must be calculated self-consistently with the G matrix and the s.p. potential U_k on the basis of the self-consistent BBG equations. It is clear from Eq. (7) that the effective force rising from the three-body force in the nuclear medium is density dependent via the defect function. A detailed description and justification of the method can be found in Refs. [17,18].

In the present calculations the Bonn B potential was adopted as V_2^{bare} [12]. Besides being a realistic interaction fitting the experimental NN scattering phase shifts, it has the advantage of being built up in terms of meson exchange as is the three-body force. Therefore the choice of the same meson parameters, that is, masses, coupling constants, and cutoffs, provides a unified treatment of two- and three-body forces as mentioned before. Details and results with this interaction are presented in Ref. [13]. In Fig. 1(a) the equations of state of pure neutron matter (PNM) and symmetric nuclear matter (SNM) are plotted. The EoS from the correlated basis theory (CBT) [7] and variational chain summation (VCS) approach [19] are also plotted for a comparison; these will be useful for our subsequent discussion of transport parameters. A strong deviation from the Brueckner calculation can be easily observed at increasing density; this is much more sizable for the symmetry energy plotted in Fig. 1(b). The symmetry energy affects the neutron star transport properties, because it essentially determines the isospin composition of the core.

In the Brueckner theory the in-medium NN cross section is obtained by replacing the T matrix with the G matrix and the in-vacuum level density with the in-medium one. This definition is supported by the property of the G matrix to reduce to the T matrix in the zero-density limit, as can be seen from BBG equation [Eq. (5)].

In the case of pure neutron matter the neutron-neutron cross section in the center-of-mass frame is written as

$$\sigma_{nn}(E,\theta) = \frac{m^{*2}}{16\pi^2\hbar^4} \sum_{SS_zS_z'} \left|G^S_{S_zS_z'}(\theta) + (-1)^S G^S_{S_zS_z'}(\pi-\theta)\right|^2 \cdot \tag{8}$$

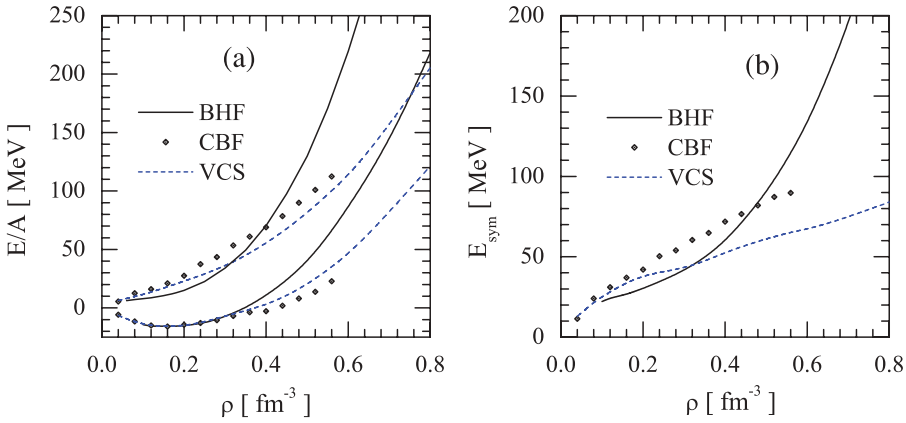

FIG. 1. (Color online) (a) Energy per particle in pure neutron matter and symmetric nuclear matter. (b) Symmetry energy, calculated as the difference between the neutron and the symmetric nuclear matter energies. The diamonds represent the results obtained using the correlated-base function (CBF) approximation with Fermi gas states [7]; the dashed lines represent the results obtained using the variational chain summation (VCS) [19].

The prefactor is the square of the level density at the Fermi energy, where in the AK approximation mainly particle transitions are assumed to occur. The medium renormalization of the nucleon mass to values much less than the unit, as shown in Fig. 2, reduces the level density with respect to the free Fermi gas value. As a consequence, the in-medium cross section also gets reduced. The additional medium effect, which is incorporated in the G matrix, is due to Pauli blocking, which prevents the particles from scattering into occupied states. In Fig. 3(a) the in-medium neutron-neutron cross section at the laboratory energy $E = 100$ MeV, obtained from Eq. (8), is compared to the corresponding free one. The forward and backward angles are sizably suppressed because the low momentum transfer transitions are forbidden by the Pauli principle, so that the differential cross section becomes more and more isotropic at increasing density. In addition, its magnitude is reduced; this is a common feature of all predictions based on microscopic approaches. In all curves the angular distribution is symmetric around 90°, since the cross section section is antisymmetrized for identical particles. In Fig. 3(b) the neutron-neutron cross section in various baryon environments is reported. It is worth noticing that it is completely isotropic in β-stable matter.

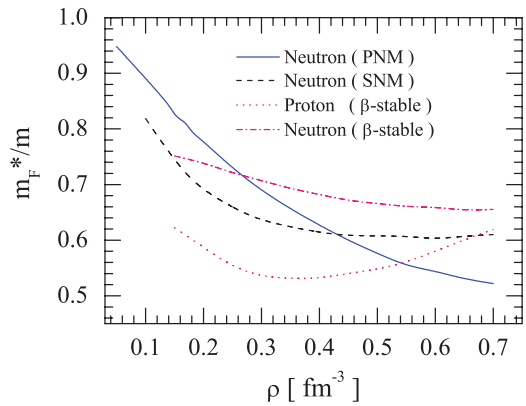

FIG. 2. (Color online) Density dependence of the neutron effective mass in pure neutron matter (solid line) and symmetric nuclear matter (dashed line). Proton (dotted line) and neutron (dot-dashed line) effective masses for beta-stable nuclear matter are also plotted.

In nuclear matter, besides neutron-neutron scattering, neutron-proton scattering must be considered. In this case the cross section is

$$\sigma_{np}(E,\theta) = \frac{m^{*2}}{16\pi^2\hbar^4} \sum_{SS_zS_z'} \left|G^S_{S_zS_z'}(\theta)\right|^2. \tag{9}$$

In Fig. 3(c) the corresponding cross sections are depicted for symmetric nuclear matter and β-stable matter. A common feature to all cases is the medium suppression, but a difference is to be noticed in the angular distribution. The enhancement in the backward direction of σ_{np} is a signature of the anisotropic behavior of the tensor force in the SD partial wave of the angular momentum expansion, giving the dominant contribution to the neutron-proton interaction [20,21].

In the core of neutron stars the neutron and proton composition is determined by the condition of equilibrium with leptons (electrons and muons), by assuming total charge neutrality. Thus for a given total baryonic density the proton and neutron fractions are determined by the chemical equilibrium condition

$$\mu_n - \mu_p = 4\beta E_{\rm sym} = \mu_e, \tag{10}$$

where μ_n, μ_p, and μ_e are the chemical potential of neutrons, protons, and electrons (with muons omitted for simplicity), respectively. The electron chemical potential is determined by the charge neutrality with protons, by assuming the electrons to form a free Fermi gas. The crucial property is the density dependence of the symmetry energy, which determines the imbalance between proton and neutron fractions. In general a nuclear system in such a state is strongly isospin asymmetric. As a consequence, the calculations of the transport coefficients must be extended to asymmetric nuclear matter. Equation (9) for the neutron-proton cross section is to be replaced by the following one:

$$\sigma_{np}(E,\theta) = \frac{1}{16\pi^2\hbar^4}\left(\frac{2m_n^*m_p^*}{m_n^*+m_p^*}\right)^2 \sum_{SS_zS_z'} \left|G^S_{S_zS_z'}(\theta)\right|^2. \tag{11}$$

For small asymmetries the isospin effect on the "reduced" effective mass is of the order of β^2, because $m_n^* \approx m_0^* + \beta m$ and $m_p^* \approx m_0^* - \beta m$, where m_0^* is the effective mass [20,22] in symmetric nuclear matter.

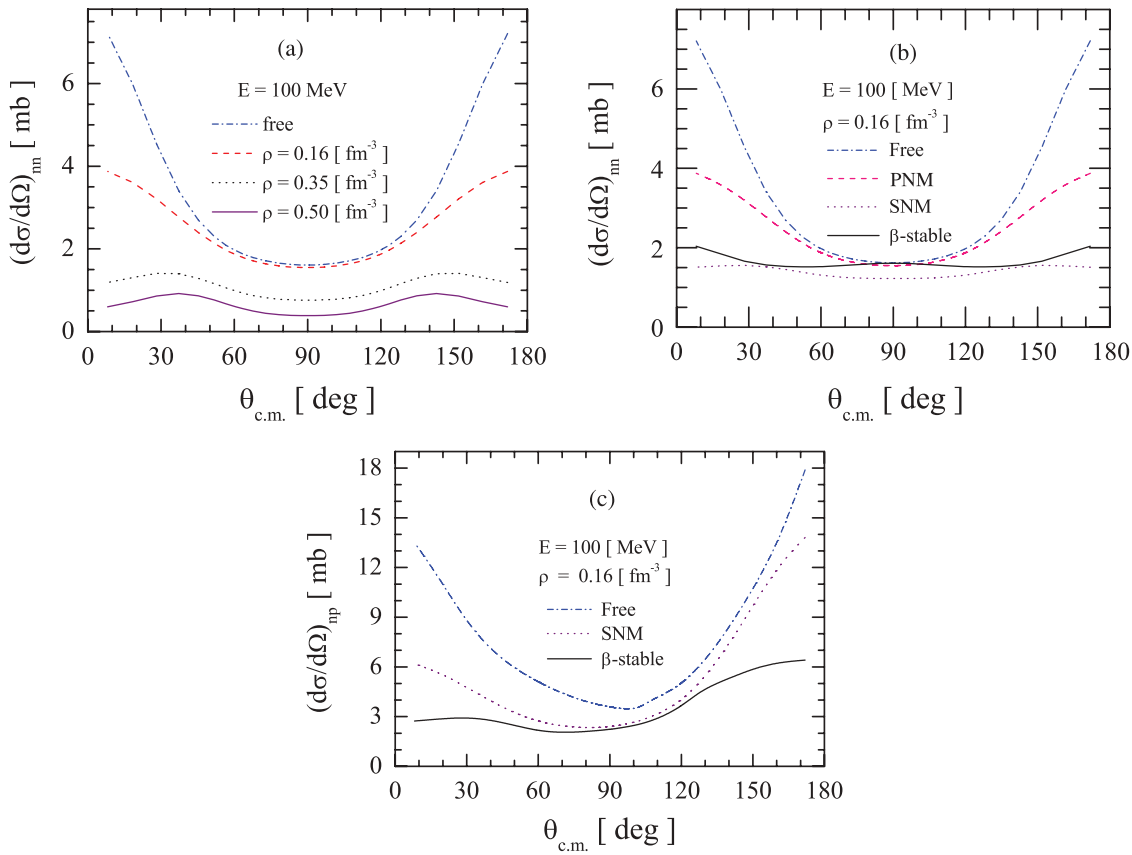

FIG. 3. (Color online) (a) Neutron-neutron differential cross sections in pure neutron matter. (b) Neutron-neutron differential cross section in pure neutron matter, symmetric, and β-stable nuclear matter. (c) Neutron-proton differential cross section in pure neutron matter, symmetric nuclear matter, and β-stable nuclear matter. The free cross section is also plotted for comparison.

IV. NUMERICAL RESULTS AND COMPARISON WITH OTHER CALCULATIONS

The shear viscosity η versus density was calculated for the three different nuclear matter configurations considered (i.e., neutron matter, symmetric nuclear matter, and β-stable asymmetric nuclear matter). In Fig. 4(a) the neutron and proton viscosities from free and in-medium cross sections are plotted versus density in the case of β-stable nuclear matter. At low total density the difference between neutrons and protons is about three orders of magnitude because the proton fraction is quite small, but it reduces to only one order of magnitude at high density where the proton fraction becomes 30% of the total density. As expected, both viscosities, corresponding to free and in-medium cross section, are increasing with density, and the medium enhancement turns out to be quite large indeed. In Fig. 4(b) the neutron viscosity in pure neutron, symmetric nuclear, and β-stable matter is plotted and the medium effects are also emphasized by the comparison with the free case. The medium effect is a strong enhancement of η, mainly as a consequence of the reduction of the level density, more pronounced for β-stable matter and less for symmetric nuclear matter. Comparing neutron matter and β-stable matter, we see that the values are very close to each other in the low-density range, where β-stable matter is essentially made of neutrons, then they deviate for the increasing weight of the proton fraction, according to the β-stability condition [see Fig. 3 and Eq. (10)].

Figure 4(c) shows the comparison among various microscopic calculations. The data from Benhar and Carbone [11], available up to a maximum range 0.3 fm^{-3}, differ from the present calculation for the different neutron-to-proton composition of β-stable nuclear matter. In that case the proton fraction, at the same total density, is larger, as a consequence of a larger symmetry energy (curve CBF in Fig. 1), and thus the influence on the neutron viscosity by the neutron-proton cross section turns out to be bigger. The data from Shternin and Yakovlev [10] were obtained from the constant effective mass approximation ($m^*/m = 0.8$ in the plot), which is not viable for the effective mass gradual quenching at higher density. The result is that the neutron viscosity is underestimated and it turns out to be smaller than the electron viscosity. The opposite happens in the present as well as the Benhar and Carbone calculation, as shown in Fig. 4(c). Therefore the electron viscosity would definitely be immaterial in the study of the energy dissipation.

The thermal conductivity κ was also calculated according to Eq. (3). The results for the various nuclear matter configurations are reported in Fig. 5. Again the medium corrections are emphasized by plotting the κ values obtained with in-vacuum and in-medium cross sections. In Fig. 5(b) the present results

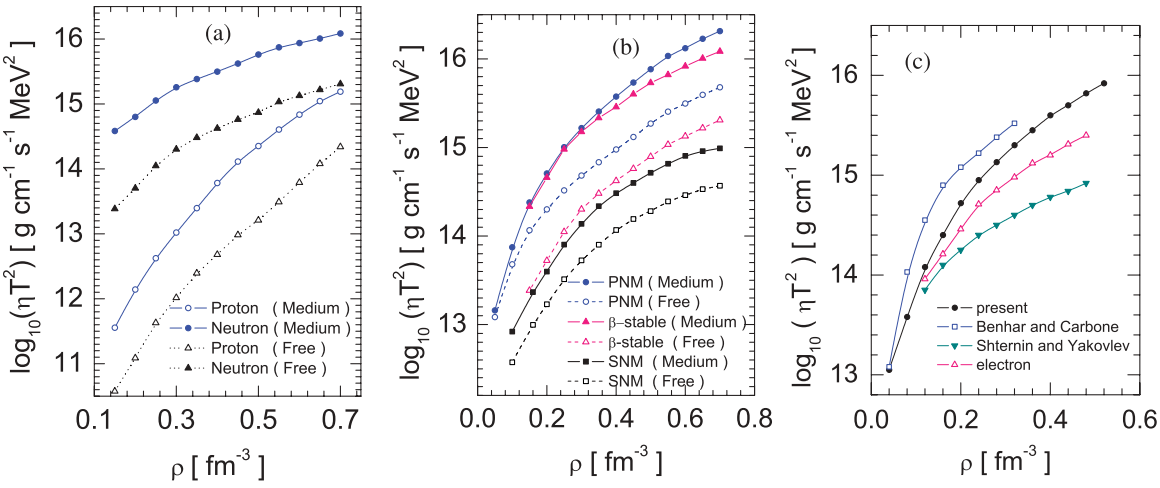

FIG. 4. (Color online) Shear viscosity from the Brueckner theory. (a) Neutron and proton shear viscosity in β-stable nuclear matter. (b) Neutron viscosity in all considered states. (c) Comparison of the Brueckner neutron viscosity with other calculations (see text) and with the electron viscosity, in β-stable nuclear matter.

are compared with the two aforementioned models [7]. To assess the extent of variations one must take into account that in this case the scale is quite different from that of Fig. 4(c). In any case the good agreement among the different models for pure neutron conductivity confirms that the deviations can only be traced to the different isospin dependence.

The transport parameters, viscosity and thermal conductivity, calculated for β-stable nuclear matter can be used to determine the respective time scales of energy dissipation, τ_V and τ_T. This requires integration of $\eta(\rho)$ and $\kappa(\rho)$ weighted with the density profile $\rho(r)$ of a given neutron star configuration. The latter can be obtained by solving the Tolman-Oppenheimer-Volkov (TOV) equation with a given equation of state of nuclear matter. Simplified expressions for the time scales governing the energy dissipation from nonradial oscillations can be derived for a quasiuniform density model [23]:

$$\tau_V^{-1} = (l-1)(2l+1)\frac{\eta}{\rho R^2}, \tag{12}$$

$$\tau_T^{-1} = 0.0034\frac{l^3(2l+1)}{l-1}\frac{\kappa T}{G\rho^2 R^4}, \tag{13}$$

where R is the radius of the star and ρ is the density calculated as the ratio between the mass M and the volume $4\pi R^3/3$. The parameter l is the angular momentum of the nonradial oscillation Y_{lm} (where in the following we consider $l = m = 2$). As discussed in Ref. [23], Eqs. (12) and (13) underestimate the values for the transport parameters within

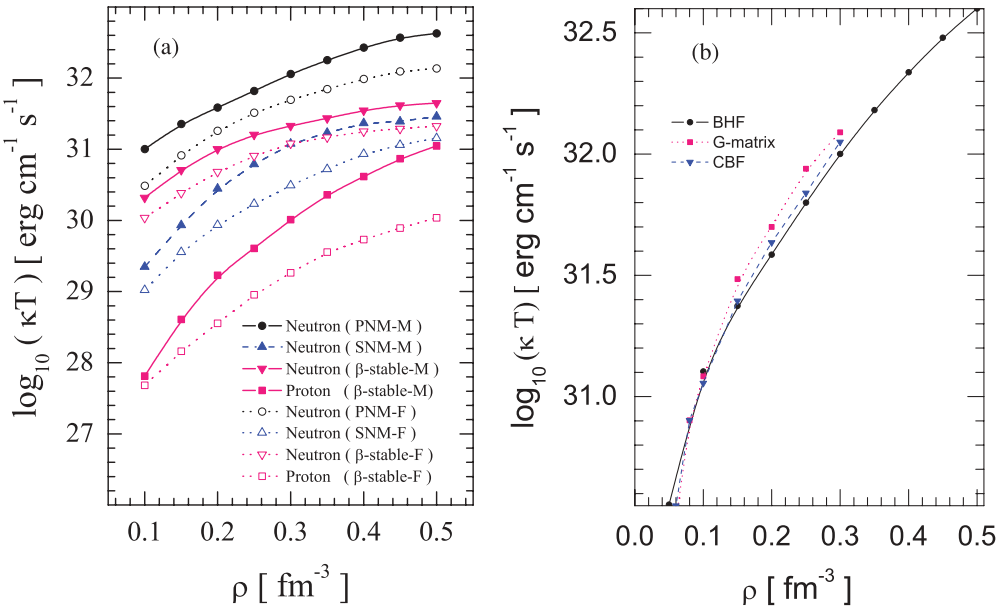

FIG. 5. (Color online) (a) Thermal conductivity from the Brueckner theory in all considered states. (b) Comparison of the thermal conductivity in pure neutron matter between the BHF approximation and two other recent calculations (see text).

TABLE I. Nonlinear mode ($l = m = 2$) damping time scale for energy dissipation induced by neutron viscosity in neutron stars.

$M/M_\odot$	R(Km)	ρ(g/cm^3) $\times 10^{14}$	t_v(s)
0.8	12.8	1.8	1865
1.4	12.5	3.4	1680
1.8	12.2	4.7	883
2.3	11.0	8.25	317

a factor about 10, because the constant-mass approximation smoothes out their increase at higher densities. In Table I the damping time scales of Y_{22} nonradial modes are reported for a number of neutron star mass-radius configurations. The neutron star configurations are taken from Ref. [24], where the TOV equation was solved by using the equation of state derived from the same BHF approximation as for the in-medium cross sections. The low-temperature results show that, within the aforementioned uncertainty of the constant-mass approximation, the time scale for energy dissipation induced by the neutron shear viscosity could be of the same order of magnitude as the time scale associated with gravitational waves (10–100 s), at least at high density. The proton contribution is much less important, since the proton partial density is much less than the total density. In other words the instability driven by gravitation radiation could be prevented by the shear viscosity dissipation in cold neutron stars. To confirm such a statement, a more accurate calculation is to be performed by means of the viscosity integration weighted with the neutron star density profiles $\rho(r)$, $0 \leqslant r \leqslant R$. In contrast, the high-temperature time scales are too large by several orders of magnitude ($\tau_V \approx 10^{13}$–10^{14} s, at $T = 3 \times 10^{11}$ K) and no help can be expected from superfluidity since the critical temperature is much less than the newborn star temperature.

The energy dissipation induced by thermal conductivity τ_T can be calculated from Eq. (12) for a nonradial mode $l = 2$. At temperature $T = 10^6$ K it is about $10^3\tau_V$ and it increases at higher temperature. Therefore its effect on the damping can be neglected, in agreement with other calculations [23].

V. CONCLUSIONS

The transport parameters, shear viscosity and thermal conductivity, of neutron stars have been calculated in the framework of the BHF approximation with two- and three-body forces. Both forces are described, in a unified treatment, by the one-boson exchange model with the meson parameters of the realistic Bonn B potential. In the Brueckner theory the in-medium NN cross sections are calculated by replacing the in-vacuum scattering amplitude with the G matrix and the nucleon bare mass with the effective mass. The in-medium strong effective mass renormalization, which affects the level density in the entrance and exit channels, is mainly responsible for the strong deviation of the in-medium NN scattering cross sections from the scattering in free space. The main result is a remarkable enhancement of the transport coefficients. This effect had been well known for several decades, but only recent *ab initio* calculations provide reliable quantitative estimates in domains of nuclear matter that do not benefit from direct empirical constraints. The underlying many-body approaches, in fact, are based on realistic NN interactions without free parameters, and they are able to calculate on the same footing both the equation of state of nuclear matter determining the composition of neutron stars as well as the transport property parameters determining the neutron star cooling and the damping of collective motions.

The calculation of the transport parameters was first performed for pure neutron matter and symmetric nuclear matter, and was then extended to β-stable nuclear matter for the sake of application to neutron stars. The calculation covers a wide density range, as needed for the study of neutron star cores. The numerical results are compared with other recent *ab initio* calculations. Concerning the shear viscosity, the BHF prediction is such that the neutrons give a contribution larger than the electrons, in contrast to the Shternin and Yakovlev calculation [10], where the constant effective mass approximation is adopted. However, the different density dependence of the symmetry energy is responsible for the different shear viscosity obtained by Benhar and Carbone [11] in β-stable configurations.

A preliminary estimate of time scales of nonradial mode damping shows that only in cold stars are the dissipation times from viscosity comparable to the gravitational radiation time, whereas the effect of thermal conduction is negligible. But these results should be confirmed by more accurate calculations beyond the constant-density approximation. Such calculations are on the way.

To interpret the spin and thermal evolution, the neutron stars have been assumed to be in a superfluid state, which could deeply influence their transport properties as well. But the recent calculations of the neutron-neutron and proton-proton gaps indicate that the proton $^1S_0$ pairing is present only in a restricted region of low density, where the proton fraction in β equilibrium with neutrons is quite small [25], and the high-density neutron gap from the channel $^3PF_2$ is so small that it could be easily suppressed by even weak polarization effects [26]. Despite this theoretical uncertainty, the onset of superfluidity is supported by the phenomenology, and its role in the damping of collective modes should be clarified.

For the application of the transport properties to neutron stars, one should also include strange components in the β-stable nuclear matter. In fact the strange particle fractions increase with density in the inner core, where they can contribute up to 20% of the total baryonic matter [27]. In the case of hybrid stars quark matter can compete with baryons; therefore the contribution to transport properties of quarks must be considered with a consistent treatment of the hadron-to-quark transition [24]. The last two research issues, superfluidity and transport properties of nonnucleonic components, are presently under investigation.

ACKNOWLEDGMENTS

H.F.Z is very grateful to the nuclear theory group for valuable discussions at LNS-INFN, where the work is done. This work is supported by the Natural Science Foundation of China (Grant Nos. 10775061, 10875152, 10875151, 10975064,

and 10740420550), by the Fundamental Research Fund for Physics and Mathematics of Lanzhou University (Grant No. LZULL200805), by the Fundamental Research Funds for the Central Universities (Grant No. lzujbky-2009-21), by the CAS Knowledge Innovation Project No. KJCX-SYW-N02, by the Major State Basic Research Developing Program of China (2007CB815004), and by the European Commission under Grant No. CN/ASIA-LINK/008(94791).

[1] E. Flowers and N. Itoh, Astrophys. J. **206**, 218 (1976); **230**, 847 (1979).
[2] A broad literature can be found in *Exotic States of Nuclear Matter and Neutron Stars*, Proceedings International Symposium EXOCT07, edited by U. Lombardo *et al.* (World Scientific, Singapore, 2008).
[3] U. Lombardo and H.-J. Schulze, in *Physics of Neutron Star Interiors*, Lecture Notes in Physics Vol. 578, edited by D. Blaschke, N. K. Glendenning, and A. Sedrakian (Springer-Verlag, Berlin, 2001), pp. 30–54.
[4] W. Zuo, U. Lombardo, H. J. Schulze, and Z. H. Li, Phys. Rev. C **74**, 014317 (2006).
[5] An extensive reference list on the in-medium NN. cross section can be found in H. F. Zhang, Z. H. Li, U. Lombardo, P. Y. Luo, F. Sammarruca, and W. Zuo, Phys. Rev. C **76**, 054001 (2007).
[6] A. D. Sedrakian, D. Blaschke, G. Roepke, and H. Schulz, Phys. Lett. B **338**, 111 (1994).
[7] O. Benhar and M. Valli, Phys. Rev. Lett. **99**, 232501 (2007).
[8] O. Benhar, A. Polls, M. Valli, and I. Vidaña, Phys. Rev. C **81**, 024305 (2010).
[9] D. A. Baiko and P. Haensel, Acta Phys. Pol. B **30**, 1097 (1999).
[10] P. S. Shternin and D. G. Yakovlev, Phys. Rev. D **78**, 063006 (2008).
[11] O. Benhar and A. Carbone, arXiv:0912.0129v1 [nucl-th].
[12] R. Mechleidt, K. Holinde, and Ch. Elster, Phys. Rep. **149**, 1 (1987); R. Machleidt, Adv. Nucl. Phys. **19**, 189 (1989).
[13] Z. H. Li, U. Lombardo, H. J. Schulze, and W. Zuo, Phys. Rev. C **77**, 034316 (2008).
[14] A. A. Abrikosov and I. M. Khalatnikov, Sov. Phys. JETP **5**, 887 (1957); Rep. Prog. Phys. **22**, 329 (1959).
[15] G. A. Brooker and J. Sykes, Phys. Rev. Lett. **21**, 279 (1968).
[16] J. Sykes and G. A. Brooker, Ann. Phys. (NY) **56**, 1 (1970).
[17] P. Grange, A. Lejeune, M. Martzolff, and J. F. Mathiot, Phys. Rev. C **40**, 1040 (1989).
[18] W. Zuo, A. Lejeune, U. Lombardo, and J. F. Mathiot, Eur. Phys. J. A **14**, 469 (2002); Nucl. Phys. A **706**, 418 (2002).
[19] A. Akmal, V. R. Pandharipande, and D. G. Ravenhall, Phys. Rev. C **58**, 1804 (1998).
[20] W. Zuo, L. G. Cao, B. A. Li, U. Lombardo, and C. W. Shen, Phys. Rev. C **72**, 014005 (2005).
[21] D. Alonso and F. Sammarruca, Phys. Rev. C **67**, 054301 (2003).
[22] G. Q. Li, R. Machleidt, and R. Brockmann, Phys. Rev. C **45**, 2782 (1992).
[23] C. Cutler and L. Lindblom, Astrophys. J. **314**, 234 (1987).
[24] G. X. Peng, A. Li, and U. Lombardo, Phys. Rev. C **77**, 065807 (2008).
[25] W. Zuo and U. Lmbardo, Phys. At. Nucl. **72**, 1359 (2009).
[26] W. Zuo, C. X. Cui, U. Lombardo, and H. J. Schulze, Phys. Rev. C **78**, 015805 (2008).
[27] M. Baldo, G. F. Burgio, and H. J. Schulze, Phys. Rev. C **61**, 055801 (2000).